*Energy Fuels* **2010,** *24,* 3589–3594 · DOI:10.1021/ef100402g
Published on Web 05/25/2010

energy&fuels
article

# Comparing Laser Desorption/Laser Ionization Mass Spectra of Asphaltenes and Model Compounds

Hassan Sabbah,*[,†] Amy L. Morrow,[†] Andrew E. Pomerantz,[‡] Oliver C. Mullins,[‡] Xiaoli Tan,[§] Murray R. Gray,[§] Khalid Azyat,[∥] Rik R. Tykwinski,[∥] and Richard N. Zare[†]

[†]*Department of Chemistry, Stanford University, Stanford, California 94305,* [‡]*Schlumberger-Doll Research, Cambridge, Massachusetts 02139,* [§]*Department of Chemical Engineering, University of Alberta, Edmonton, Alberta T6G 2H1, Canada, and* [∥]*Department of Chemistry, University of Alberta, Edmonton, Alberta T6G 2G2, Canada*

*Received April 1, 2010. Revised Manuscript Received May 11, 2010*

The molecular-mass distribution of the asphaltene fraction of petroleum is rapidly becoming more constrained, but the molecular architecture remains poorly understood. Two types of molecular structures have been proposed to be representative of asphaltenes: the "island" model and the "archipelago" model. Here, nine compounds were synthesized on the basis of pyrene, representing both types of models. These compounds were analyzed using two-step laser desorption/laser ionization mass spectrometry ($L^2MS$), and the compounds were classified into three groups based on their fragmentation behavior in this typically soft ionization technique. The first two groups, denoted "highly fragmented" and "variably fragmented", include eight of the nine studied compounds. The masses of fragment ions from the "highly fragmented" group were too small for these specific compounds to dominate the asphaltenes. The fragmentation behavior of the variably fragmented group was inconsistent with $L^2MS$ spectra of asphaltene samples; thus, these specific compounds can be excluded from being dominant in asphaltenes. The third group, "highly stable", contains a single model compound with properties in the aromatics class fraction and exhibits a behavior consistent with previously observed asphaltene samples, namely, inappreciable fragmentation as a function of laser pulse energy used. Although suggestive, no definitive conclusion can be reached as to the dominant molecular architecture of asphaltenes without the study of how more model compounds behave under $L^2MS$.

## Introduction

Asphaltenes, defined as the fraction of petroleum that is insoluble in *n*-pentane or *n*-heptane but soluble in toluene or benzene, are a very complex mixture of polycyclic aromatic hydrocarbons (PAHs) variably substituted with alkyl groups, heteroatoms (N, S, and O), and metals (Ni and V). Although asphaltene elemental compositions are well-known and a consensus is rapidly forming regarding a typical asphaltene molecular-mass distribution,[1−8] controversy still remains regarding the molecular architecture of what are the dominating asphaltene components. Two models have been advanced to describe the structures of molecules present in asphaltenes. In the "archipelago" model[9,10] several aromatic moieties are linked through aliphatic bridges, which potentially contain heteroatoms. An alternative proposed architecture is the "island" model,[11,12] which consists of one polyaromatic core with pendant aliphatic chains that may contain heteroatoms as well. The question has been posed: Which, if either, of these two models is the better description of the structure of asphaltene molecules?

To address this question, nine model compounds were synthesized at the University of Alberta, as listed in Table 1. At Stanford University, the laser desorption/laser ionization mass spectrum ($L^2MS$) of each compound was recorded

*To whom correspondence should be addressed. Telephone: +650-723-4318. E-mail: sabbah@stanford.edu.

(1) Hortal, A. R.; Hurtado, P.; Martinez-Haya, B.; Mullins, O. C. Molecular-weight distributions of coal and petroleum asphaltenes from laser desorption/ionization experiments. *Energy Fuels* **2007**, *21* (5), 2863–2868.

(2) Hortal, A. R.; Martinez-Haya, B.; Lobato, M. D.; Pedrosa, J. M.; Lago, S. On the determination of molecular weight distributions of asphaltenes and their aggregates in laser desorption ionization experiments. *J. Mass Spectrom.* **2006**, *41* (7), 960–968.

(3) Klein, G. C.; Kim, S.; Rodgers, R. P.; Marshall, A. G. Mass spectral analysis of asphaltenes. I. Compositional differences between pressure-drop and solvent-drop asphaltenes determined by electrospray ionization Fourier transform ion cyclotron resonance mass spectrometry. *Energy Fuels* **2006**, *20* (5), 1965–1972.

(4) Klein, G. C.; Kim, S.; Rodgers, R. P.; Marshall, A. G.; Yen, A. Mass spectral analysis of asphaltenes. II. Detailed compositional comparison of asphaltenes deposit to its crude oil counterpart for two geographically different crude oils by ESI FT-ICR MS. *Energy Fuels* **2006**, *20* (5), 1973–1979.

(5) Martinez-Haya, B.; Hortal, A. R.; Hurtado, P.; Lobato, M. D.; Pedrosa, J. M. Laser desorption/ionization determination of molecular weight distributions of polyaromatic carbonaceous compounds and their aggregates. *J. Mass Spectrom.* **2007**, *42* (6), 701–713.

(6) Pomerantz, A. E.; Hammond, M. R.; Morrow, A. L.; Mullins, O. C.; Zare, R. N. Asphaltene molecular-mass distribution determined by two-step laser mass spectrometry. *Energy Fuels* **2009**, *23*, 1162–1168.

(7) Rodgers, R. P.; Schaub, T. M.; Marshall, A. G. Petroleomics: MS returns to its roots. *Anal. Chem.* **2005**, *77* (1), 20A–27A.

(8) Mullins, O. C. The modified Yen model. *Energy Fuels* **2010**, *24*, 2179–2207.

(9) Murgich, J.; Abanero, J. A.; Strausz, O. P. Molecular recognition in aggregates formed by asphaltene and resin molecules from the Athabasca oil sand. *Energy Fuels* **1999**, *13* (2), 278–286.

(10) Sheremata, J. M.; Gray, M. R.; Dettman, H. D.; McCaffrey, W. C. Quantitative molecular representation and sequential optimization of athabasca asphaltenes. *Energy Fuels* **2004**, *18* (5), 1377–1384.

(11) Groenzin, H.; Mullins, O. C. Molecular size and structure of asphaltenes from various sources. *Energy Fuels* **2000**, *14*, 677–684.

(12) Zhao, S. Q.; Kotlyar, L. S.; Sparks, B. D.; Woods, J. R.; Gao, J. S.; Chung, K. H. Solids contents, properties and molecular structures of asphaltenes from different oilsands. *Fuel* **2001**, *80* (13), 1907–1914.

 

**Table 1. Designations and Structures of the Nine Model Compounds Examined during This Work for Their Similarity to Asphaltene**

| Name | Structure |
|---|---|
| 1,4-dipyren-1-yl-butane (P-*n*Bu-P) | 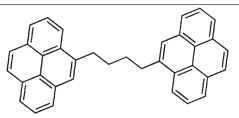 |
| 2,6-Bis(2-pyren-1-yl-ethyl)-pyridine (P-2,6-PyrP) | 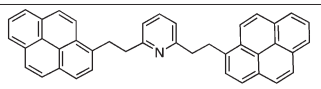 |
| 2,5-Bis(2-pyren-1-yl-ethyl)-thiophene (PThP) | 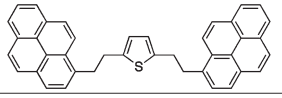 |
| 5,5'-Bis(2-pyren-1-yl-ethyl) -2,2'-bithiophene (PBiThP) | 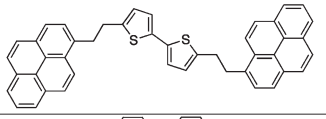 |
| 2,7-Bis(2-pyren-1-yl-ethyl)- 9,9-diethyl-9H-fluorene (PFP) | 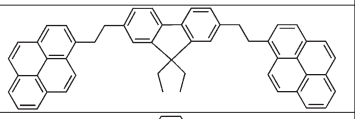 |
| 1,4-Bis(2-pyren-1-yl-ethyl)-benzene (P-*p*PhP) | 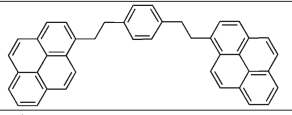 |
| 4,4'-Bis(2-pyren-1-yl-ethyl) -2,2'-bipyridine (PBP) | 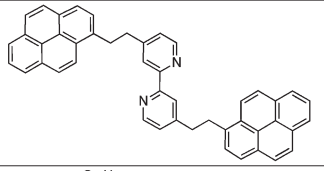 |
| 1,6-didecyl pyrene (DDP) | 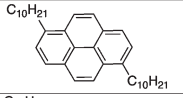 |
| 1,3,6,8-tetradecyl pyrene (TDP) | 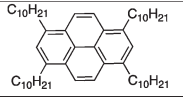 |

under the same conditions that $L^2MS$ were taken of asphaltenes. By this means, we hope to find which model compounds mimic more closely asphaltene molecules. It is hoped that this information may put some constraints on what could be the dominant components of asphaltenes.

In $L^2MS$, an infrared laser pulse is used to desorb neutral species from the surface of a solid sample via rapid heating. This plume is free of ions because the pulse energy of the infrared desorption laser (~0.1 eV) is far below the ionization threshold of any potential asphaltene molecule (~7 eV). Aggregation is suppressed because of many factors,[6,13] including the absence of ion-induced dipole forces. After an appropriate time delay, an ultraviolet laser pulse intersects the plume and ionizes species containing aromatic groups. Gas-phase ionization results in a low-density cloud of ions.[14] These ions are then mass-analyzed using a reflectron time-of-flight mass spectrometer.

In what follows, we describe the synthesis of the model compounds, discuss the mass spectrometric analysis, and compare the behavior of the different model compounds to that of asphaltenes.

(13) Pomerantz, A. E.; Hammond, M. R.; Morrow, A. L.; Mullins, O. C.; Zare, R. N. Two-step laser mass spectrometry of asphaltenes. *J. Am. Chem. Soc.* **2008**, *130* (23), 7216–7217.

(14) Hahn, J. H.; Zenobi, R.; Zare, R. N. Subfemtomole quantitation of molecular adsorbates by two-step laser mass spectrometry. *J. Am. Chem. Soc.* **1987**, *109* (9), 2842–2843.

## Experimental Section

**Model Compound Sample Preparation.** *General Considerations.* 1-Ethynylpyrene, 2,7-dibromo-9,9′-diethylfluorene, and 5,5′-diiodo-2,2′-bithiophene were synthesized as previously reported.[15−17] 2,6-Dibromopyridine, 2,5-diiodothiophene, and 1,4-diiodobenzene were purchased from commercial suppliers. Tetrahydrofuran (THF) was dried over Na/benzophenone prior to use. A positive pressure of nitrogen gas was essential to the success of all Pd-catalyzed cross-coupling reactions between 1-ethynylpyrene and diidodo- or dibromoarene.

*General Procedure.* Under an atmosphere of nitrogen, 1-ethynylpyrene (2.2 mmol) was added to a deoxygenated solution of the appropriate diidodo- or dibromoarene (1.0 mmol) and diisopropylamine (10 mL) in THF (50 mL); the solution was held under an atmosphere of nitrogen. $PdCl_2(PPh_3)_2$ (70 mg, 0.10 mmol) and CuI (38 mg, 0.20 mmol) were sequentially added, and the solution was stirred at reflux until thin-layer chromatography (TLC) analysis no longer showed the presence of starting material (typically 2−24 h). After the reaction was judged complete, it was cooled to room temperature and the solvents were removed *in vacuo*. The resulting solid was washed with MeOH (5 × 20 mL), hexane (5 × 20 mL), and water (5 × 20 mL); it was then filtered and dried *in vacuo*.

This crude product and THF (50 mL) were added to a glass hydrogenation tube, and 10% Pd/C (50 mg) was added. The tube was placed in an autoclave; the autoclave was purged 3 times with hydrogen; and the hydrogen pressure was regulated at 1200 psi for ca. 3 days. Once hydrogenation was complete, the resulting inhomogeneous mixture was filtered to remove the catalyst and the THF was removed *in vacuo*. The resulting crude solid was purified via column chromatography (silica gel 60, 230−400 mesh) to afford the desired product; typical yields are 50−70%.

In nearly all cases, the major impurity from the reaction sequence above is P-*n*Bu-P, the result of homocoupling of 1-ethynylpyrene during the initial cross-coupling reaction. Compound P-*n*Bu-P ($R_f$ = 0.45; 4:1 hexane/$CHCl_3$) can be identified as the less polar fraction in comparison to the desired products, P-2,6-PyrP ($R_f$ = 0.11; 4:1 hexane/$CHCl_3$), PFP ($R_f$ = 0.13; 4:1 hexane/$CHCl_3$), PThP ($R_f$ = 0.22; 7:3 hexane/$CHCl_3$), PBiThP ($R_f$ = 0.12; 4:1 hexane/$CHCl_3$), or P-*p*PhP ($R_f$ = 0.17; 4:1 hexane/$CHCl_3$).

The synthesis of PBP was described previously.[18] Synthesis of TDP and DDP was accomplished in three steps: bromination of pyrene, coupling of the side chains via an alkyne intermediate, and then catalytic hydrogenation. For TDP, 1,3,6,8-tetrabromopyrene was made by adding excess bromine to a solution of pyrene in nitrobenzene at 120 °C for 12 h. To make 1,6-dibromopyrene, 1.8 equiv of bromine was added to a solution of pyrene in carbon tetrachloride. The alkyne-substituted intermediates were made by Sonogashira coupling, with the addition of 1-decyne to a solution of bromopyrene in piperidine with $PdCl_2(PPh_3)_2$ and CuI, and then refluxing under argon at 80 °C for 10 h. After cooling, the solvent was removed on a rotary evaporator. The residue was acidified with concentrated HCl and extracted with $CH_2Cl_2$. The organic phase was dried over

(15) Hissler, M.; Harriman, A.; Khatyr, A.; Ziessel, R. Intramolecular triplet energy transfer in pyrene−metal polypyridine dyads: A strategy for extending the triplet lifetime of the metal complex. *Chem.—Eur. J.* **1999**, *5* (11), 3366–3381.

(16) Kannan, R.; He, G. S.; Yuan, L. X.; Xu, F. M.; Prasad, P. N.; Dombroskie, A. G.; Reinhardt, B. A.; Baur, J. W.; Vaia, R. A.; Tan, L. S. Diphenylaminofluorene-based two-photon-absorbing chromophores with various π-electron acceptors. *Chem. Mater.* **2001**, *13* (5), 1896–1904.

(17) Li, Z. H.; Wong, M. S.; Fukutani, H.; Tao, Y. Full emission color tuning in bis-dipolar diphenylamino-endcapped oligoarylfluorenes. *Chem. Mater.* **2005**, *17* (20), 5032–5040.

(18) Tan, X. L.; Fenniri, H.; Gray, M. R. Pyrene derivatives of 2,2′-bipyridine as models for asphaltenes: Synthesis, characterization, and supramolecular organizations. *Energy Fuels* **2008**, *22* (2), 715–720.

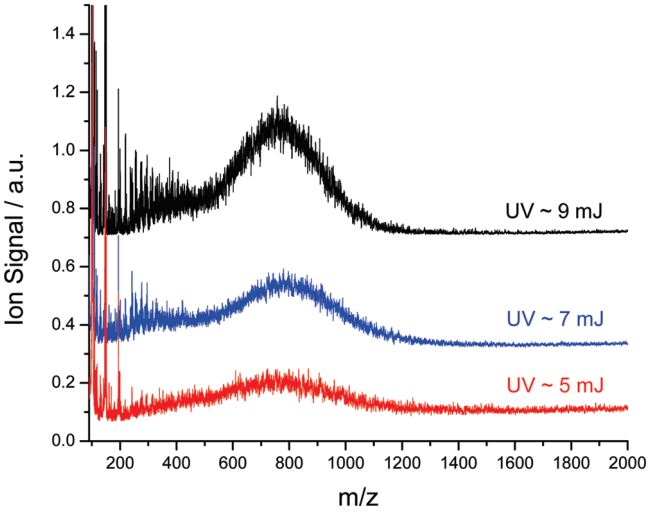


**Figure 1.** $L^2MS$ spectra of BG5 asphaltene powder recorded at different ionization pulse energies, showing no change in molecular-mass distribution but intensity increasing with the laser pulse energy.

$MgSO_4$, and the solvent was removed under reduced pressure. The crude product was recrystallized from ethanol−benzene to give 1,3,6,8-tetradecynylpyrene for TDP and 1,6-didecynylpyrene for DDP. The alkynyl pyrenes were hydrogenated with Pd−carbon in THF over 7 days under 56 psi at room temperature. The crude product was crystallized in *n*-hexane.

To prepare the samples for mass spectrometric analysis, they were dissolved to 1 mg/mL solutions in toluene. From each solution, a 20 $\mu$L drop was spotted onto a glass sample platter. These samples were introduced into the system via a vacuum interlock, after allowing 1 h for the toluene to evaporate in ambient conditions.

**Two-Step Laser Desorption/Laser Ionization Mass Spectrometry Technique.** The $L^2MS$ is similar to the one described previously.[14,19] The asphaltene molecular-weight distribution as detected by $L^2MS$ is insensitive to instrumental parameters, such as desorption and ionization laser pulse energies and time delays.[6,13] For example, the independence of the observed asphaltene molecular-mass distribution from the ionization laser pulse energy is illustrated in Figure 1. High desorption laser pulse energies promote volatilization of high-molecular-weight species while avoiding plasma-phase aggregation. The volatilization/ionization process in $L^2MS$ is typically soft, such that the spectra of aromatic species are dominated by singly charged parent ions. This behavior was observed in the following compound classes: PAHs, porphyrins,[20] amino acids,[21] and aerosols.[22]

In the $L^2MS$ experiments, the sample is mounted on a XYZ manipulator and then aligned 2 mm below the center of the ion extraction region of the mass spectrometer. Once the sample is introduced inside the mass spectrometer, analysis is delayed for 15−30 min to allow for evaporation of any residual solvent, which would otherwise produce an intense background. A germanium dichroic mirror is used to direct visible light from inside the sample chamber to a charge-coupled device (CCD) camera to visualize the sample in the extraction region of the instrument. A pulse of infrared (IR) light ($\lambda$ = 10.6 $\mu$m) from a $CO_2$ laser (Alltech AL 882 APS) is employed to desorb the molecules adsorbed on the surface of the glass platter. This pulse has a 120 ns full width at half-maximum (fwhm) Gaussian peak with a 4 $\mu$s tail. The laser beam is focused to a spot of 50 $\mu$m diameter, employing a Cassegrainian microscope objective (Ealing Optics, 15×). The typical pulse energy used for this experiment is 5−10 mJ/pulse, resulting in a fluence of 200 J $cm^{-2}$. Pulsed laser light focused on a highly localized area results in a heating rate of about $10^8$ K/s,[23,24] inducing a much more rapid temperature rise than resistive heating (10 K/s). This rapid heating process favors desorption over decomposition,[24] allowing this technique to desorb many neutral species with minimal fragmentation . The combination of the XYZ manipulator and the CCD camera provides the ability to identify visually and probe a fresh surface of the sample with each laser shot.

Desorbed neutral molecules from the platter surface form a plume in the extraction region during a delay time of 10−50 $\mu$s. This plume is subsequently irradiated perpendicularly by the fourth harmonic (266 nm) of a Nd:YAG laser (Spectra Physics DCR11; 10 ns pulse width; 10 Hz repetition rate), which causes 1 + 1 resonance-enhanced multiphoton ionization (REMPI) of desorbed molecules that absorb at this wavelength. This wavelength is selected to ionize organic species containing an aromatic group. During this work, the time delay between the two laser steps and the pulse energy of the both laser pulses were varied. Gaseous deuterated toluene (MW = 100 Da) present in the sample chamber serves as an internal standard to convert from time-of-flight (TOF) to the mass/charge ratio.

Finally, the created ions are mass-separated in a home-built reflectron TOF mass spectrometer using a modified Wiley−McLaren geometry.[25] A dual microchannel plate set in a Chevron configuration (MCPs; 20 $cm^2$ active area; Burle Electro-Optics, Sturbridge, MA) coupled with a large collector anode (Galileo TOF-4000) is used as a detector. The generated ion signal is amplified by a fast pre-amplifier (Ortec 9326) and a timing filter (Ortec 474), after which it is displayed on a digital oscilloscope (LeCroy 9450). The resulting signal is averaged within the oscilloscope for a series of 50 pairs of $CO_2$ and Nd:YAG laser shots for each recorded spectrum.

## Results

Mass spectra for the nine model compounds listed in Table 1 were obtained using the $L^2MS$ instrument described above. In this section, we present the results of these measurements by dividing the compounds into three categories depending upon their fragmentation behavior. Additionally, we present spectra of typical petroleum asphaltenes for comparison. These experiments were carried out at different desorption and ionization pulse energies as well as time delays. As stated above, $L^2MS$ spectra of asphaltenes exhibit little dependence upon desorption laser energy and time delay; increasing the ionization laser pulse energy results in greater signal intensity

(19) Kovalenko, L. J.; Philippoz, J. M.; Bucenell, J. R.; Zenobi, R.; Zare, R. N. Organic chemical analysis on a microscopic scale using two-step laser desorption multiphoton ionization mass spectrometry. *Space Sci. Rev.* **1990**, *56*, 191–195.

(20) Betancourt, S. S.; Ventura, G. T.; Pomerantz, A. E.; Viloria, O.; Dubost, F. X.; Zuo, J.; Monson, G.; Bustamante, D.; Purcell, J. M.; Nelson, R. K.; Rodgers, R. P.; Reddy, C. M.; Marshall, A. G.; Mullins, O. C. Nanoaggregates of asphaltenes in a reservoir crude oil and reservoir connectivity. *Energy Fuels* **2008**, *23*, 1178–1188.

(21) Engelke, F.; Hahn, J. H.; Henke, W.; Zare, R. N. Determination of phenylthiohydantoin-amino acids by two-step laser desorption multiphoton ionization. *Anal. Chem.* **1987**, *59* (6), 909–912.

(22) Kalberer, M.; Morrical, B. D.; Sax, M.; Zenobi, R. Picogram quantitation of polycyclic aromatic hydrocarbons adsorbed on aerosol particles by two-step laser mass spectrometry. *Anal. Chem.* **2002**, *74* (14), 3492–3497.

(23) Sherman, M. G.; Kingsley, J. R.; McIver, R. T.; Hemminger, J. C. Laser-induced thermal desorption with Fourier transform mass spectrometric detection. In *Catalyst Characterization Science*; American Chemical Society (ACS): Washington, D.C., 1985; ACS Symposium Series, Vol. 288, Chapter 21, pp 238−251.

(24) Deckert, A. A.; George, S. M. Heating rates required for laser-induced thermal desorption studies of surface reaction kinetics. *Surf. Sci.* **1987**, *182* (1−2), L215–L220.

(25) Wiley, W. C.; McLaren, I. H. Time-of-flight mass spectrometer with improved resolution. *Rev. Sci. Instrum.* **1955**, *26* (12), 1150–1157.

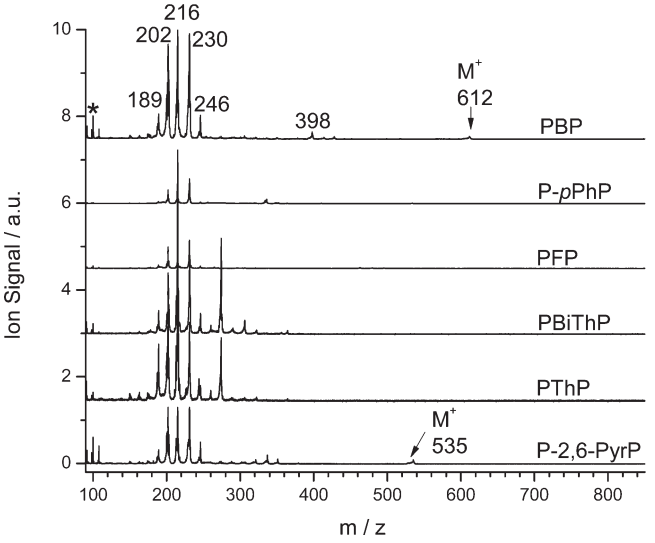


**Figure 2.** $L^2MS$ spectra ($CO_2$ energy, 5 mJ/pulse; UV energy, 7 mJ/pulse) of six candidate "asphaltene-like" model compounds consisting of two pyrene cores connected by substituted alkyl chain structures. All show similar fragmentation behavior. Peaks indicated by an asterisk are from the internal standard, toluene-$d_8$ (MW = 100).

without altering the shape of the mass spectrum, as shown by the different traces in Figure 1.

**Highly Fragmented Model Compounds.** The first class of these model compounds shows dominant fragment ion peaks at all instrumental parameters studied here. This class consists of six bridged pyrene derivatives (PBP, P-2,6-PyrP, PThP, PBiThP, PFP, and P-*p*PhP), and their spectra are presented in Figure 2. Parent ion peaks appear at very low intensity for two model compounds (PBP and P-2,6-PyrP) and are not observed for the other four compounds in this category. The variation of instrumental parameters produces no observable differences in the mass spectra of these six compounds. For example, Figure 3 presents the mass spectra of PBP at different ionization pulse energies and demonstrates that this compound fragments extensively regardless of the ionization laser pulse energy. Additionally, Figure 4 shows no effect of changing the desorption laser pulse energy on the resulting observed mass spectra of P-2,6-PyrP.

The dominance of fragment peaks in the mass spectrum of PBP is similar to that observed in an earlier study,[26] employing laser-induced acoustic desorption (LIAD)/electron ionization (EI) in a Fourier transform ion cyclotron resonance mass spectrometer (FT-ICR MS). The most intense peaks in the spectra of these compounds appear at $m/z$ below 250, and several peaks can tentatively be assigned to pyrene and its derivatives, bearing zero, one, or two methylene groups as a side chain ($-CH_2-$, $m/z$ 14).

**Variably Fragmented Model Compounds.** The second class of these compounds shows fragmentation behavior dependent upon instrumental parameters. This class consists of one bridged pyrene derivative (P-*n*Bu-P) and one pyrene substituted with two terminal alkyl chains (DDP), and their spectra are represented in Figures 5 and 6, respectively. The number and intensity of the fragment peaks in the $L^2MS$ spectra of these two model compounds were found to change with various ionization laser pulse energies. These spectral differences are highlighted in Figure 7. For example, the $L^2MS$ mass spectra (see Figures 5 and 7) of P-*n*Bu-P recorded at different ionization laser pulse energies show a competition between parent and fragment ions. The most intense peak at all pulse energies studied appears at $m/z$ 216 and is tentatively assigned to a fragment ion consisting of pyrene with one methylene group. At low ionization laser pulse energy, the parent ion is the second most intense peak in the spectrum and fragment ion peaks at $m/z$ other than 216 are barely observable. As the ionization laser pulse energy is increased, the relative intensities of other fragment ion peaks grow. At the highest ionization laser pulse energy studied, their intensities are comparable to that of the parent ion (see Figure 7).

The other compound (DDP) in this class is similar in structure to the proposed "island" model of asphaltenes. This compound also shows variable fragmentation behavior depending upon the ionization laser pulse energy (see Figure 6). At low ionization laser pulse energy, the parent ion peak is the only observable peak in the mass spectrum.

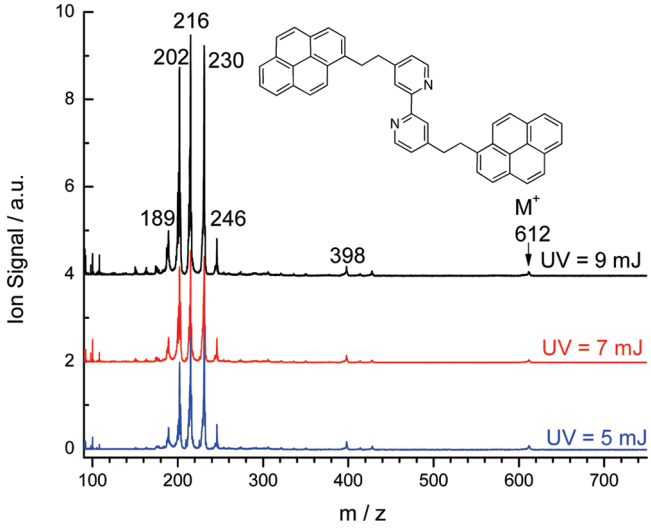


**Figure 3.** Mass spectra of PBP at different UV ionization laser pulse energies.

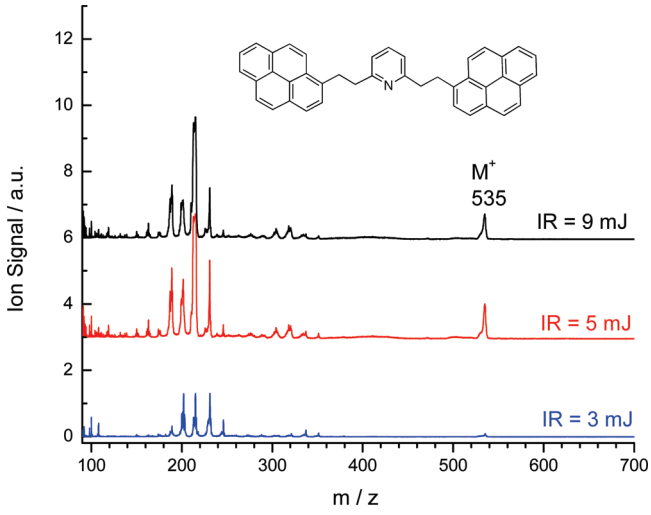


**Figure 4.** Mass spectra of P-2,6-PyrP repeated at different desorption laser pulse energies.

(26) Pinkston, D. S.; Duan, P.; Gallardo, V. A.; Habicht, S. C.; Tan, X. L.; Qian, K. N.; Gray, M.; Mullen, K.; Kenttamaa, H. I. Analysis of asphaltenes and asphaltene model compounds by laser-induced acoustic desorption/fourier transform ion cyclotron resonance mass spectrometry. *Energy Fuels* **2009**, *23*, 5564–5570.

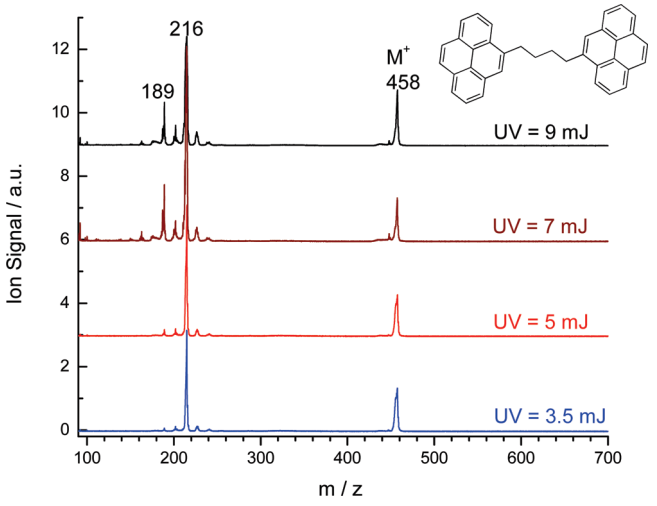


**Figure 5.** $L^2MS$ mass spectra of P-*n*Bu-P achieved at different ionization laser pulse energies ranging from 3.5 to 9 mJ/pulse.

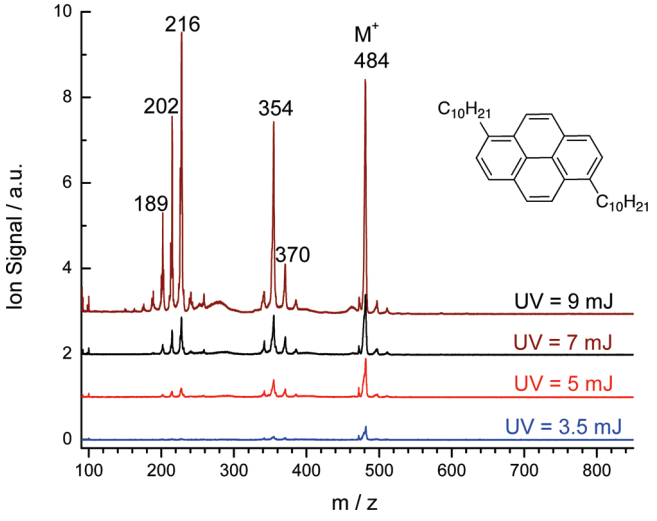


**Figure 6.** Mass spectra of DDP showing the fragmentation behavior of this pyrene derivative at different ionization laser pulse energies.

As the ionization laser pulse energy is increased, the relative intensities of fragment ion peaks grow. At the highest ionization laser pulse energy studied, several fragment ion peaks appear at comparable intensity to the parent ion peak.

**Highly Stable Model Compounds.** The third class of these compounds shows dominant parent ion peaks and no dependence upon instrumental parameters. This class includes one compound (TDP) consisting of one pyrene substituted with four terminal alkyl chains, and the spectra are presented in Figure 8. The $L^2MS$ spectra of this compound show highly stable behavior regarding all of the varied experimental conditions. For example, Figure 8 presents the mass spectra of TDP at different ionization laser pulse energies and demonstrates that the parent ion peak dominates regardless of the ionization laser pulse energy. A similar behavior was observed in the work of Pinkston et al.,[26] employing LIAD/EIMS.

## Discussion

**Highly Fragmented Model Compounds.** (1 + 1) REMPI typically provides soft ionization, in which the parent ions

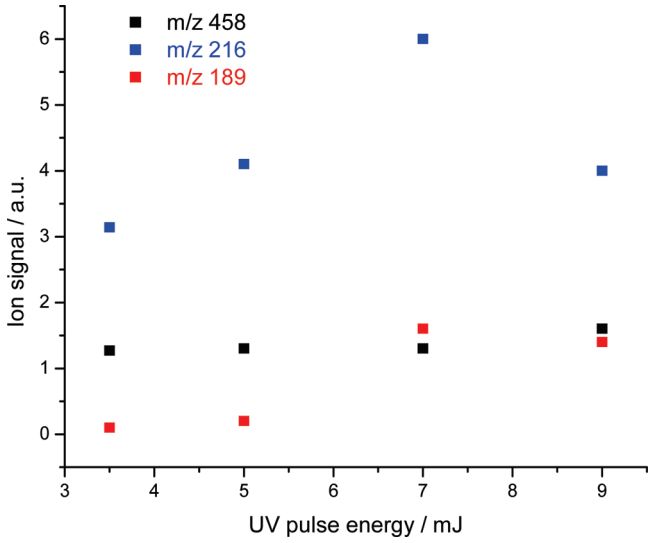


**Figure 7.** Peak intensity variations of P-*n*Bu-P parent ions (*m*/*z* 458) and fragment ions at *m*/*z* 216 and 189 with the variation of the UV pulse energy.

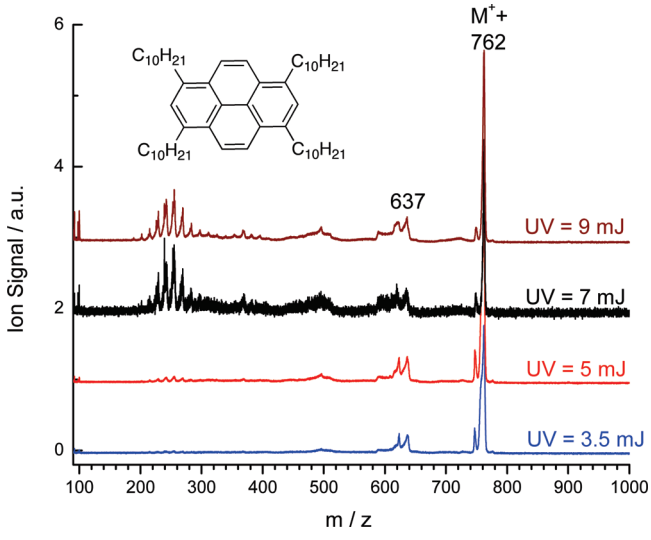


**Figure 8.** Mass spectra of TDP repeated at different ionization laser pulse energies.

dominate the mass spectra,[14,21,27−31] as observed in the following classes of chemicals: PAHs, porphyrins,[20] and amino acids.[21] However, $L^2MS$ spectra of the compounds in class one (PBP, P-2,6-PyrP, PThP, PBiThP, PFP, and P-*p*PhP) were dominated by fragment ions at all experimental conditions.

(27) Grotemeyer, J.; Boesl, U.; Walter, K.; Schlag, E. W. A general soft ionization method for mass spectrometry: Resonance-enhanced multiphoton ionization of biomolecules. *Org. Mass Spectrom.* **1986**, *21* (10), 645–653.
(28) Grotemeyer, J.; Boesl, U.; Walter, K.; Schlag, E. W. Biomolecules in the gas-phase. 2. Multiphoton ionization mass spectrometry of angiotensin-I. *Org. Mass Spectrom.* **1986**, *21* (9), 595–597.
(29) Lightner, D. A.; Quistad, G. B.; Irwin, E. Hydrogen rearrangements in mass spectra of alkylbenzenes. *Appl. Spectrosc.* **1971**, *25* (2), 253–258.
(30) Tembreull, R.; Lubman, D. M. Pulsed laser desorption of biological molecules in supersonic beam mass spectrometry with resonant two-photon ionization detection. *Anal. Chem.* **1987**, *59* (8), 1082–1088.
(31) Zare, R. N. Laser chemical analysis. *Science* **1984**, *226* (4672), 298–303.

The observed fragmentation is potentially caused by the presence of the alkyl chain bridges linking the two pyrene cores, because alkyl chains are expected to be cleaved relatively easily.[29,32,33] Assignment of the main fragment peaks as pyrene substituted with 0−2 $CH_2$ groups is consistent with this expectation. Isolated PAH ions typically dissipate the delivered excess energy through two competing processes,[33,34] infrared emission and unimolecular decay. As Jochims et al.[33,34] argue persuasively, PAH ions containing less than 30−40 carbon atoms dissociate rather than radiate in the infrared. Given the molecular weight of the model compounds, we can exclude infrared relaxation from further discussion. On the other hand, PAH ions with energy in excess of a chemical bond are expected to dissociate, but the time scale for dissociation must not exceed the time required for extraction to detect fragment ions. If unimolecular dissociation occurs in the field-free drift region, the signal will be recorded near the mass of the parent ion. Dissociation occurring after the extraction region but ahead of the reflectron will produce perturbations in the resulting mass spectrum, broadening the observed parent ion peak but producing no individual fragment ion peaks. The dominance of fragment ion peaks observed here suggest that the rate of unimolecular fragmentation exceeds the time it takes the ions to be accelerated through the potential drop region. Additionally, the dominant fragment peaks are observed around $m/z$ 216, an $m/z$ range where asphaltenes produce little signal.

**Variably Fragmented Model Compounds.** The model compounds P-*n*Bu-P and DDP exhibit variable fragmentation behavior with different ionization laser pulse energies. Fragmentation likely involves cleaving a bond in the pendant aliphatic chains, as consistent with the assignment of the fragment ions. Although P-*n*Bu-P and DDP have similar fragmentation behavior, they have different molecular structures: P-*n*Bu-P contains two pyrene cores linked by an aliphatic bridge and represents an "archipelago" structure; DDP contains a single pyrene core with two pendant aliphatic chains, representing an "island" structure. At the lowest ionization laser pulse energy studied (3.5 mJ/pulse), a fragment ion peak dominates the $L^2$MS spectrum of P-*n*Bu-P, while the parent ion peak dominates the $L^2$MS spectrum of DDP.

The analyses of these compounds speak to the ability of the $L^2$MS method to observe parent ions without fragmentation. The data show that the current $L^2$MS does not give reliable estimates of the parent ion mass of the structures in both the highly fragmented and variably fragmented groups.

**Highly Stable Model Compound.** The resistance of TDP to fragmentation at all experimental conditions was an unexpected discovery given the observed variable fragmentation in the structurally similar DDP. The structural difference between DDP and TDP is the presence of two additional alkyl chains on the latter. We suggest that the stability of this compound can be attributed to its longer unimolecular dissociation lifetime. This lifetime exceeds the time required (approximately 0.5 $\mu$s) for the molecule to enter the field-free region of the TOF, after which resulting fragments will be detected near the parent ion $m/z$ value. As a result, the parent ion peak dominates the $L^2$MS mass spectra. Additionally, the intense parent ion peak ($m/z$ 762) appears at a location near the most likely observed mass detected in $L^2$MS spectra of asphaltenes ($m/z$ 600−800).

## Conclusion

In this work, we compare the $L^2$MS spectra of nine model compounds to those of asphaltenes. Model compounds were divided into three classes based on their fragmentation behavior in $L^2$MS. The first class produced dominant fragmentation peaks that are centered close to $m/z$ 216 at all instrumental parameters studied here, which we classify as highly fragmenting compounds. Because asphaltenes exhibit low signal intensity below $m/z$ 250 in $L^2$MS spectra, these specific compounds (PBP, P-2,6-PyrP, PThP, PBiThP, PFP, and P-*p*PhP) are not dominant in asphaltenes.

The second class of model compounds exhibit variable fragmentation, which depends upon the pulse energy of the ionization laser. This class includes one compound representative of the "archipelago" model (P-*n*Bu-P) and one compound representative of the "island" model (DDP). Because asphaltenes do not exhibit variable fragmentation behavior in $L^2$MS spectra, these specific compounds are not dominant in asphaltenes.

The final class of model compounds shows $L^2$MS spectra dominated by parent ion peaks at all instrumental parameters studied here. Additionally, the parent ion peak is located near the most likely observed molecular mass of asphaltenes. This class includes one compound whose structure is representative of the "island" model (TDP). The similarity between the $L^2$MS spectra of TDP and the $L^2$MS spectra of asphaltenes indicates that TDP behaves under $L^2$MS in the same manner as asphaltenes. However, it is important to note that the solubility of this compound in *n*-heptane and its adhesion to silica gel place it in the saturates, aromatics, resins, and asphaltenes (SARA) aromatics fraction. Clearly, many more model compounds must be studied to define the nature of the asphaltene molecular architecture.

(32) Gray, M. R.; McCaffrey, W. C. Role of chain reactions and olefin formation in cracking, hydroconversion, and coking of petroleum and bitumen fractions. *Energy Fuels* **2002**, *16* (3), 756–766.

(33) Jochims, H. W.; Baumgartel, H.; Leach, S. Structure-dependent photostability of polycyclic aromatic hydrocarbon cations: Laboratory studies and astrophysical implications. *Astrophys. J.* **1999**, *512* (1), 500–510.

(34) Jochims, H. W.; Ruhl, E.; Baumgartel, H.; Tobita, S.; Leach, S. Size effects on dissociation rates of polycyclic aromatic hydrocarbon cations: Laboratory studies and astrophysical implications. *Astrophys. J.* **1994**, *420* (1), 307–317.